Available online at www.sciencedirect.com
ScienceDirect
Developmental Biology 302 (2007) 66–79
DEVELOPMENTAL BIOLOGY
www.elsevier.com/locate/ydbio

A critical role for the *EphA3* receptor tyrosine kinase in heart development

Lesley J. Stephen [a], Amy L. Fawkes [a], Adam Verhoeve [a], Greg Lemke [b], Arthur Brown [a,*]

[a] *BioTherapeutics Research Group, The John P. Robarts Research Institute, and The University of Western Ontario, London, Ontario, Canada N6A 5K8*
[b] *Molecular Neurobiology Laboratory, The Salk Institute for Biological Studies, La Jolla, CA 92037, USA*

Received for publication 29 May 2006; revised 23 August 2006; accepted 24 August 2006
Available online 30 August 2006

Abstract

Eph proteins are receptor tyrosine kinases that control changes in cell shape and migration during development. We now describe a critical role for EphA3 receptor signaling in heart development as revealed by the phenotype of *EphA3* null mice. During heart development mesenchymal outgrowths, the atrioventricular endocardial cushions, form in the atrioventricular canal. This morphogenetic event requires endocardial cushion cells to undergo an epithelial to mesenchymal transformation (EMT), and results in the formation of the atrioventricular valves and membranous portions of the atrial and ventricular septa. We show that *EphA3* knockouts have significant defects in the development of their atrial septa and atrioventricular endocardial cushions, and that these cardiac abnormalities lead to the death of approximately 75% of homozygous $EphA3^{-/-}$ mutants. We demonstrate that *EphA3* and its ligand, *ephrin-A1*, are expressed in adjacent cells in the developing endocardial cushions. We further demonstrate that $EphA3^{-/-}$ atrioventricular endocardial cushions are hypoplastic compared to wildtype and that $EphA3^{-/-}$ endocardial cushion explants give rise to fewer migrating mesenchymal cells than wildtype explants. Thus our results indicate that EphA3 plays a crucial role in the development and morphogenesis of the cells that give rise to the atrioventricular valves and septa.

Keywords: Eph; Ephrin; Endocardial cushion; Atrial septum; Heart development; EMT

Introduction

Eph receptors constitute the largest subfamily of receptor tyrosine kinases by far (Klein, 2001; Noren and Pasquale, 2004; Wilkinson, 2000). Clustering and activation of Eph receptors occur upon binding to their membrane-bound ephrin ligands (Davis et al., 1994). A strikingly complementary pattern of expression between Ephs and ephrins in apposed cellular compartments has been observed in the developing rhombomeres (Cooke and Moens, 2002), along neural crest migration pathways (Krull et al., 1997) and in tissues throughout the entire developing mouse embryo (Gale et al., 1996). There is also now considerable biochemical and genetic evidence for bi-directional signaling between Eph proteins and the ephrins, with the latter acting as signaling 'receptors', such that Eph/ephrin engagement activates signaling pathways in both interacting cells (Huai and Drescher, 2001; Mellitzer et al., 1999; Xu et al., 1999).

In contrast to most other receptor tyrosine kinases, activation of Eph receptors does not typically lead to a proliferative response in receptor-expressing cells, but rather to changes in cell shape and movement (Klein, 2001). Eph receptors and ephrins have been extensively characterized as mediating axon-repelling events (Drescher et al., 1995; Winslow et al., 1995), but have also been shown to provide attractive signals (Knoll et al., 2001) and signals that mediate cell adhesion (Davy and Robbins, 2000; Lawrenson et al., 2002; Miao et al., 2000). A large body of evidence supports a role for Eph receptors and ephrins in axon guidance (Brown et al., 2000; Knoll and Drescher, 2002; Wilkinson, 2000), neural tube closure (Holmberg et al., 2000), neural crest migration (Krull, 1998), vascular (Adams et al., 1999), and notochord development (Naruse-Nakajima et al., 2001). Indeed, the evolutionary expansion of Eph receptors and ephrin ligands, has led to the speculation that these receptors and ligands must play important and specialized roles in patterning the vertebrate body plan (Boyd and Lackmann, 2001).

We have previously reported that *EphA3* is expressed in the embryonic brain, spinal cord, musculature, lungs, and kidneys,

* Corresponding author.
E-mail address: abrown@robarts.ca (A. Brown).

0012-1606/$ - see front matter © 2006 Elsevier Inc. All rights reserved.
doi:10.1016/j.ydbio.2006.08.058

with prominent expression in the developing heart (Kilpatrick et al., 1996). In order to study the role of *EphA3* in neurodevelopment, we generated an *EphA3* null mutant by homologous recombination in embryonic stem (ES) cells. These *EphA3*$^{-/-}$ mice failed to demonstrate abnormalities in motor neuron projection patterns but did show an increased perinatal mortality (Vaidya et al., 2003). We now report that *EphA3* and *ephrin-A1* are expressed in adjacent cells of the developing mouse heart, and that *EphA3*$^{-/-}$ mice develop debilitating endocardial cushion and atrial septal defects that lead to death in most mutants. Thus, EphA3 signaling has a previously unrecognized yet important role in cardiogenesis.

Materials and methods

Embryo and organ collection

Timed mouse mating were established with the morning of a vaginal plug defined as E0.5. For all analyses, to minimize the possible confounding contribution of slight differences in developmental age of wildtype and *EphA3*$^{-/-}$ embryos, at least 9 wildtype and 9 *EphA3*$^{-/-}$ mutants (3 embryos from 3 different litters) were analyzed. Embryonic age was verified by staging the embryos by development of the fore- and hindlimb paddles.

RNA in situ hybridization

E12.5 and E11 wildtype embryos were isolated and submersion fixed in 4% paraformaldehyde overnight. Hybridization was performed following published protocols (Schaeren-Wiemers and Gerfin-Moser, 1993). The *EphA3* probe was a 900-bp fragment from the 5′end of the gene (Kilpatrick et al., 1996); the *ephrin-A1* probe was a 337-bp fragment (nucleotides 328–665); the *NF-ATc* probe was a 387-bp fragment (nucleotides 546–933) and the Sox4 probe was a 338-bp fragment (nucleotides 328–666).

Electrocardiograms

Electrocardiograms were performed on wildtype and *EphA3*$^{-/-}$ perinatal mice. Electrodes were inserted subcutaneously in the right and left forearms and in the left hindlimb. Recordings were taken with a Grass Polygraph and the data analyzed using Powerlab software (AD Instruments, Mountain View, California).

Morphometric analysis of endocardial cushion volume measurements

Fluorescent images of phalloidin–rhodamine (Sigma)-stained serial sections (10 μm) through the entire atrioventricular cushion and ventricles were taken using Q Capture (DB2®) software. The atrioventricular endocardial cushion and ventricular regions were outlined and their cross sectional areas quantified using Image Pro Plus software. Volumes were computed as the sum of the product of cross sectional area and section thickness. Data are expressed as mean±SEM.

Cell counts in endocardial cushions

Five consecutive 10 μm serial sections from the middle of each wildtype and *EphA3*$^{-/-}$ atrioventricular endocardial cushion were stained with phalloidin–rhodamine to delineate the extent of the endocardial cushions and DAPI (4,6 diamino-2-phenylindole, Sigma) to visualize the cell nuclei. Fluorescent images were taken with Q Capture software (DB2®) and the nuclei in the atrioventricular endocardial cushion were counted by a blinded observer (crude counts). Abercrombie's equation was applied to the crude cell counts to correct for double cell counting (Abercrombie, 1946). The difference between wildtype and *EphA3*$^{-/-}$ cushion cell numbers was analyzed using the Student's *t*-test, with $P<0.05$ designated as the level of statistical significance. Data are expressed as mean±SEM.

Cell density

Serial sections through entire wildtype and *EphA3*$^{-/-}$ atrioventricular endocardial cushions were stained with phalloidin–rhodamine to delineate the extent of the endocardial cushions and DAPI to visualize the cell nuclei. Fluorescent images were taken with Q Capture software (DB2®). Image Pro Plus software was used to quantify the area of DAPI fluorescence per cushion area. The percentages of DAPI fluorescence per unit area in the endocardial cushions of wildtype and *EphA3*$^{-/-}$ were compared as a relative measure of cell density. Statistical significance was assessed by the Student's *t*-test using a significance level of $P<0.05$. Data are represented as mean±SEM.

Filamentous actin staining

To visualize filamentous actin, E12.5 wildtype and *EphA3*$^{-/-}$ atrioventricular endocardial cushion sections (20 μm) were fixed in 4% formaldehyde in PBS for 20 min at room temperature. Sections were permeabilized with 0.5% Triton X-100 in PBS for 5 min, blocked with 10% FBS in PBS and stained with 0.1 mg/ml phalloidin–rodamine for 1 h.

3D collagen gel migration assay

Atrioventricular explant cultures were performed as described (Bernanke and Markwald, 1982). Briefly, the entire atrioventricular canal and outflow tracts, including the adjacent myocardium, from wildtype and *EphA3*$^{-/-}$ E10.5 embryos were microdissected with tungsten needles and explanted onto a drained type I collagen gel (Collaborative Research). Ventricles were also microdissected and used as negative control explants. Cultures were examined and scored for mesenchymal cell invasion at 48 and 72 h using an inverted microscope with Hoffman optics. To identify migrating mesenchymal cells the microscope was focused on the surface of the gel and gradually adjusted to focus at increasing depths within the gel. The primary criterion used to identify migrating mesenchymal cells was the appearance of cells with characteristic spindle-shaped appearance below the surface of the gel (Runyan and Markwald, 1983). A blinded observer counted the number of mesenchymal cells that invaded the gel and the difference between wildtype and *EphA3*$^{-/-}$ explants was analyzed using the Student's *t*-test, with $P<0.05$ designated as the level of statistical significance. Data are expressed as mean±SEM.

Cell proliferation assay

Pregnant mice were given intraperitoneal injections with 100 μg/g body weight BrdU (Roche Applied Science) 1 h prior to sacrifice. Five consecutive transverse cryostat sections through the central region of each embryo's atrioventricular endocardial cushion were processed for immunohistochemistry using an anti-BrdU monoclonal antibody (Roche Applied Science) and signal visualized with a DAB reaction. Sections were counterstained with DAPI. DAB- and DAPI-positive nuclei were counted and expressed as a percentage of the total number of nuclei within each section. The data are expressed as mean±SEM. Student's *t*-test was used for data comparison, with $P<0.05$ designated as the level of statistical significance.

Apoptosis (TUNEL) assay

Apoptotic cells were detected on five consecutive 10 μm cryostat sections using a modified TUNEL technique (Cregan et al., 1999) by specific end-labeling of fragmented nuclear DNA with biotin–dUTP (Roche Applied Science). Biotin-labeled fragmented DNA was detected with Streptavidin-Alexa488 (Vector laboratories). Sections were counterstained with DAPI and the number of TUNEL-positive nuclei was counted and expressed as a percentage of the total number of nuclei within each section. The data are expressed as mean±SEM. Student's *t*-test was used for data comparison, with $P<0.05$ designated as the level of statistical significance.

Results

EphA3 null mutants die perinatally due to cardiac failure

We generated a line of mice that carry a null mutation in the *EphA3* gene. The construct design and screening strategy has been previously reported (Vaidya et al., 2003). Chimeric founder mice that transmitted the targeted allele were bred to 129S3Svimj mice allowing us to analyze the mutants on a pure genetic background. We observed that approximately 75% of homozygous *EphA3*$^{-/-}$ mice die within the first 2 days of life. Although the *EphA3*$^{-/-}$ newborns appeared to be well formed and to feed after birth, they quickly became cyanotic, and lethargic. At postmortem examination, the most obvious abnormality observed in these mice was the enlargement of their atria (Figs. 1A, C, D) which were engorged with blood and dilated. The atrial dilatation suggested high cardiac filling pressures in *EphA3*$^{-/-}$ hearts. To evaluate the possibility of increased venous congestion that would be expected in the face of high cardiac filling pressures, we examined *EphA3*$^{-/-}$ and

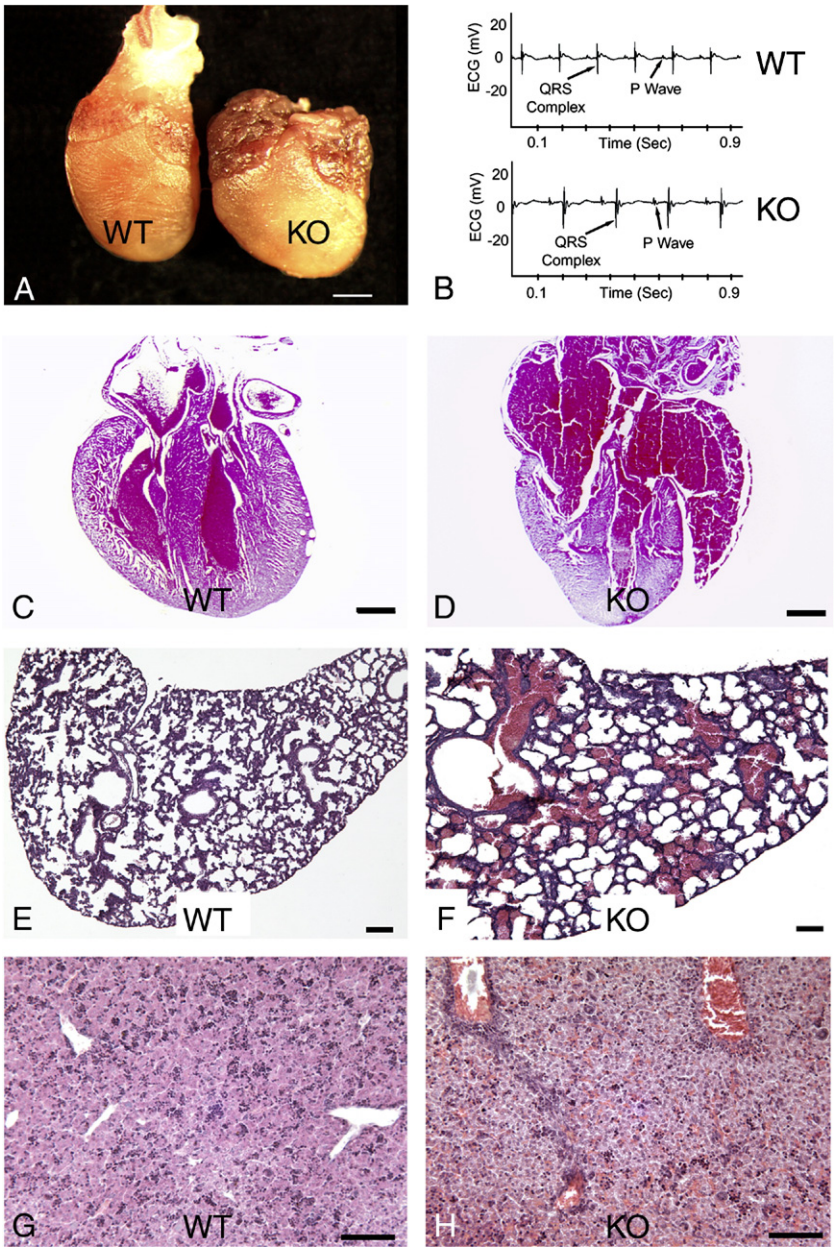

Fig. 1. Patholgical examination of wildtype and *EphA3*$^{-/-}$ P0 hearts, lungs and livers. (A, C, D) At postmortem examination, *EphA3*$^{-/-}$ P0 hearts have grossly enlarged, blood-filled atria. (E–H) Consistent with the presence of high cardiac filling pressures in *EphA3*$^{-/-}$ mice, histological examination revealed blood congestion in *EphA3*$^{-/-}$ lungs (E, F) and livers (G, H). Note specifically the presence of blood in the alveoli of *EphA3*$^{-/-}$ lungs and the venous congestion in the *EphA3*$^{-/-}$ livers. (B) The cardiac performance of *EphA3*$^{-/-}$ mice was investigated by electrocardiography. Compared to age-matched wildtype mice ($N=6$), the *EphA3*$^{-/-}$ mice ($N=11$) have a substantial bradycardia and a prolonged PR interval. RA, right atrium; LA, left atrium; RV, right ventricle; LV, left ventricle; WT, wildtype; KO, *EphA3* knockout. Scale bar 1.0 mm.

wildtype postnatal day 0 (P0) lungs and livers. This analysis revealed that the neonatal *EphA3*$^{-/-}$ lungs were poorly inflated and that their alveoli were blood-filled (Figs. 1E, F). The blood present in *EphA3*$^{-/-}$ lungs is an indication of exceedingly high cardiac filling pressures leading to capillary disruption. Significantly, *EphA3*$^{-/-}$ livers were also congested with blood as compared to wildtype (Figs. 1G, H). Though we have previously reported that *EphA3* is also expressed in the developing brain, spinal cord, lungs, kidneys and muscle (Kilpatrick et al., 1996), none of these organs showed obvious defects in the *EphA3*$^{-/-}$ mutants (aside from venous congestion) as assessed by histology.

Cardiac dysfunction in EphA3$^{-/-}$ *mutants*

Given that our analysis suggested that the *EphA3*$^{-/-}$ P0 animals were dying of cardiac failure, we investigated their cardiac performance by carrying out electrocardiography on wildtype ($N=6$) and *EphA3*$^{-/-}$ ($N=11$) P0 mice. ECGs were analyzed for mean heart rate (HR), PR interval (atrial and AV nodal conduction time), QRS interval (ventricular depolarization time), and Q–T interval (a surrogate of action potential duration). *EphA3*$^{-/-}$ mice were found to have a significant bradycardia and first-degree atrioventricular (AV) block (as evidenced by a prolonged PR interval) compared to wildtype mice. *EphA3*$^{-/-}$ mice had an average heart rate of 297±17.9 bpm while wildtype mice had an average heart rate of 396±16.3 bpm. The average PR interval (the interval between the start of the P wave and the beginning of the QRS complex) for *EphA3*$^{-/-}$ mice was 0.06±0.006 s compared to 0.04±0.005 s in wildtype mice (Fig. 1B). *EphA3*$^{-/-}$ ECGs did not reveal evidence of arrhythmia or of second- or third-degree AV conduction block.

Atrioventricular canal and septal defects in EphA3$^{-/-}$ *mutants*

Hearts from *EphA3*$^{-/-}$ P0 animals ($N=16$) that became cyanotic after birth were compared by histological analysis to age- and genetic background-matched wildtype P0 hearts ($N=10$). The most striking feature of the mutant hearts was their high degree of atrial dilatation and blood engorgement when compared to wildtype (Figs. 1,2). A possible explanation for this finding lies in the histological observation of annular dilatation in the atrioventricular valves of the EphA3 knockout mice. While wildtype left and right atrioventricular orifices were narrow and filled by their valvular leaflets, *EphA3*$^{-/-}$ atrioventricular orifices were enlarged and their valvular leaflets inadequate to close the right and left atrioventricular canals (Figs. 2A–D). To ensure that the annular dilatation seen in *EphA3*$^{-/-}$ atrioventricular valves was not due to the plane of section, we examined all serial sections from the wildtype and *EphA3*$^{-/-}$ P0 animals processed. In no case did we find *EphA3*$^{-/-}$ atrioventricular valves that were competent to close or whose leaflets overlapped as seen in wildtype sections.

The atrioventricular septum, the septum separating the right atrium from the left ventricle, was also found to be much thinner in the *EphA3* null animals than in wildtype (Figs. 2A–D). The P0 mutants that became cyanotic were also found to have a pronounced atrial septal defect (Figs. 2E, F). The atrial septum is composed of a septum primum and a septum secundum (an infolding of the dorsal wall of the atria). While an infolding representing the septum secundum was occasionally observed in *EphA3*$^{-/-}$ sections, the septum primum was either totally absent or was represented by only a thin remnant. Atrioventricular valve dilatation and septal defects were also readily observed in E16.5 *EphA3*$^{-/-}$ embryos (Figs. 2H, I).

EphA3 and ephrin-A1 expression in the developing heart

In order to understand the cardiac defects in the newborn *EphA3*$^{-/-}$ animals, we analyzed EphA3 expression during cardiogenesis. Using RNA *in situ* hybridization, we detected EphA3 mRNA as early as E10.5 in the developing atrioventricular (Fig. 3A) and outflow tract endocardial cushions (Fig. 3C), and in the mesenchymal cap of the developing septum primum at E12.5 (Fig. 3B). The endocardial cushions are mesenchymal structures that give rise to the atrioventricular valves and septa (Webb et al., 1998). RNA *in situ* hybridizations for EphA1, A2, A4, A5, A6, A7 and A8 on sections of E12.5 embryos failed to reveal cardiac expression of these EphA receptors.

Eph receptors have been shown in other systems to exert their effects by interacting with their cell surface bound ligands, often in apposed cell populations. (Gale and Yancopoulos, 1997; Gilardi-Hebenstreit et al., 1992; Smith et al., 1997). We therefore performed RNA *in situ* hybridizations at E12.5, using anti-sense riboprobes to each of the ephrin-A ligands (ephrin-A1,-A2,-A3,-A4 and -A5). Only eprhin-A1 showed cardiac expression at this developmental time-point. We found that *ephrin-A1* is specifically expressed in a set of cells that are closely apposed to cells expressing *EphA3* in both the developing outflow tract (Figs. 3C, D) and in the atrioventricular endocardial cushions (Figs. 3B, E, G). To identify the *EphA3* and *ephrin-A1*-expressing cells, RNA *in situ* hybridizations were also carried out on serial cross sections of E12.5 hearts using riboprobes to *Sox4*, a gene expressed throughout the endocardial cushions (Marco et al., 1998), and to *NF-ATc*, a marker of the endothelial lining of the endocardial cushions (Pompa et al., 1998; Ranger et al., 1998) (Figs. 3F, H). These expression studies demonstrated that *EphA3* is expressed in the mesenchymal cells of the endocardial cushions, while *ephrin-A1* is expressed in cells of the surrounding endothelial lining.

EphA3$^{-/-}$ *endocardial cushions are hypoplastic*

As described above, the annuli of the atrioventricular valves in P0 *EphA3*$^{-/-}$ mice were dilated and their atrioventricular septa hypoplastic. To determine if the *EphA3*$^{-/-}$ endocardial cushions that give rise to these valves were hypoplastic we measured the volume of the endocardial cushions from wildtype and *EphA3*$^{-/-}$ E12.5 embryos. Morphometric analyses demonstrated that *EphA3*$^{-/-}$ cushions were 28.8% smaller ($P<0.05$) than wildtype (Figs. 4A, D, G). To investigate whether this

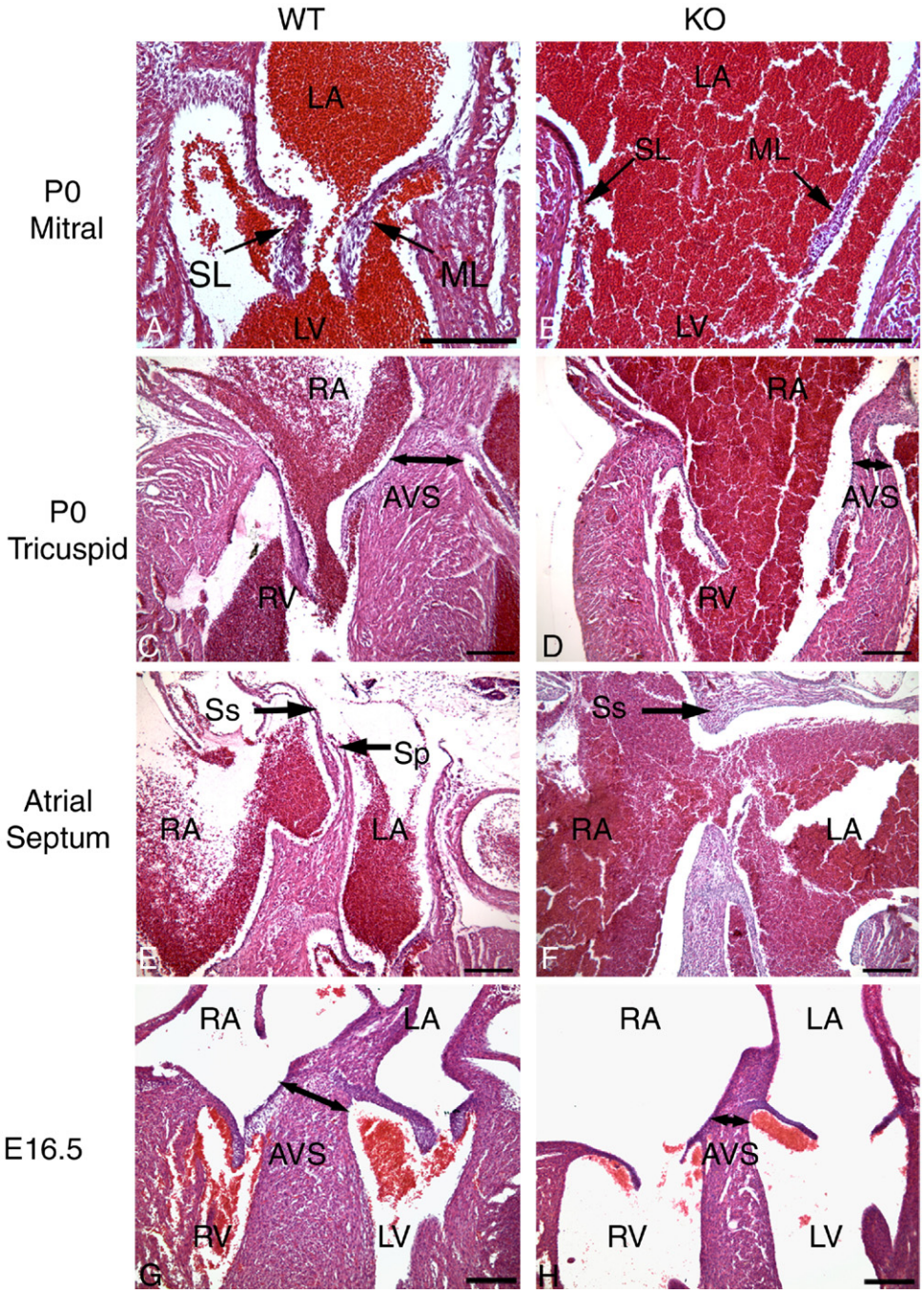

Fig. 2. Atrioventricular junction and septal abnormalities in *EphA3*$^{-/-}$ mutants. (A–D) The atrioventricular valves of P0 *EphA3*$^{-/-}$ mice (B, D) that become cyanotic and lethargic demonstrate abnormal morphology compared to wildtype controls (A, C). Note the annular dilatation (enlarged orifices) of the atrioventricular valves in the *EphA3*$^{-/-}$ mice and that the atrioventricular septum is much thinner in *EphA3*$^{-/-}$ mice than in the wildtype controls. (E, F) These *EphA3*$^{-/-}$ mice also demonstrate the almost total absence of an atrial septum that is made up of the septum primum and septum secundum. (G, H) E16.5 *EphA3*$^{-/-}$ embryos also show atrioventricular annular dilatation and reduction in the thickness of the atrioventricular septum. AVS, atrioventricular septum; RA, right atrium; RV, right ventricle; LA, left atrium; LV, left ventricle; SL, septal leaflet; ML, mural leaflet; Sp, septum primum; Ss, septum secundum; WT, wildtype; KO, *EphA3* knockout. Scale bar 0.1 mm.

reduction in size was due to a decreased number of cells in *EphA3*$^{-/-}$ endocardial cushions, we measured the area of DAPI immunofluorescence per unit area of the endocardial cushion as an indication of cell density over the entire endocardial cushion in the wildtype and *EphA3*$^{-/-}$ embryos. This analysis indicated that the cell densities in wildtype and *EphA3*$^{-/-}$ endocardial cushions were not significantly different from each other and that therefore the number of cells in *EphA3*$^{-/-}$ endocardial cushions must be approximately 28.8% lower than in wildtype. A direct cell count from the central portion of each endocardial cushion from these same embryos verified that the number of endocardial cushion cells per section was reduced by 29% in *EphA3*$^{-/-}$ embryos (Figs. 4B, E, H). To investigate whether the entire *EphA3*$^{-/-}$ heart was smaller than wildtype we measured

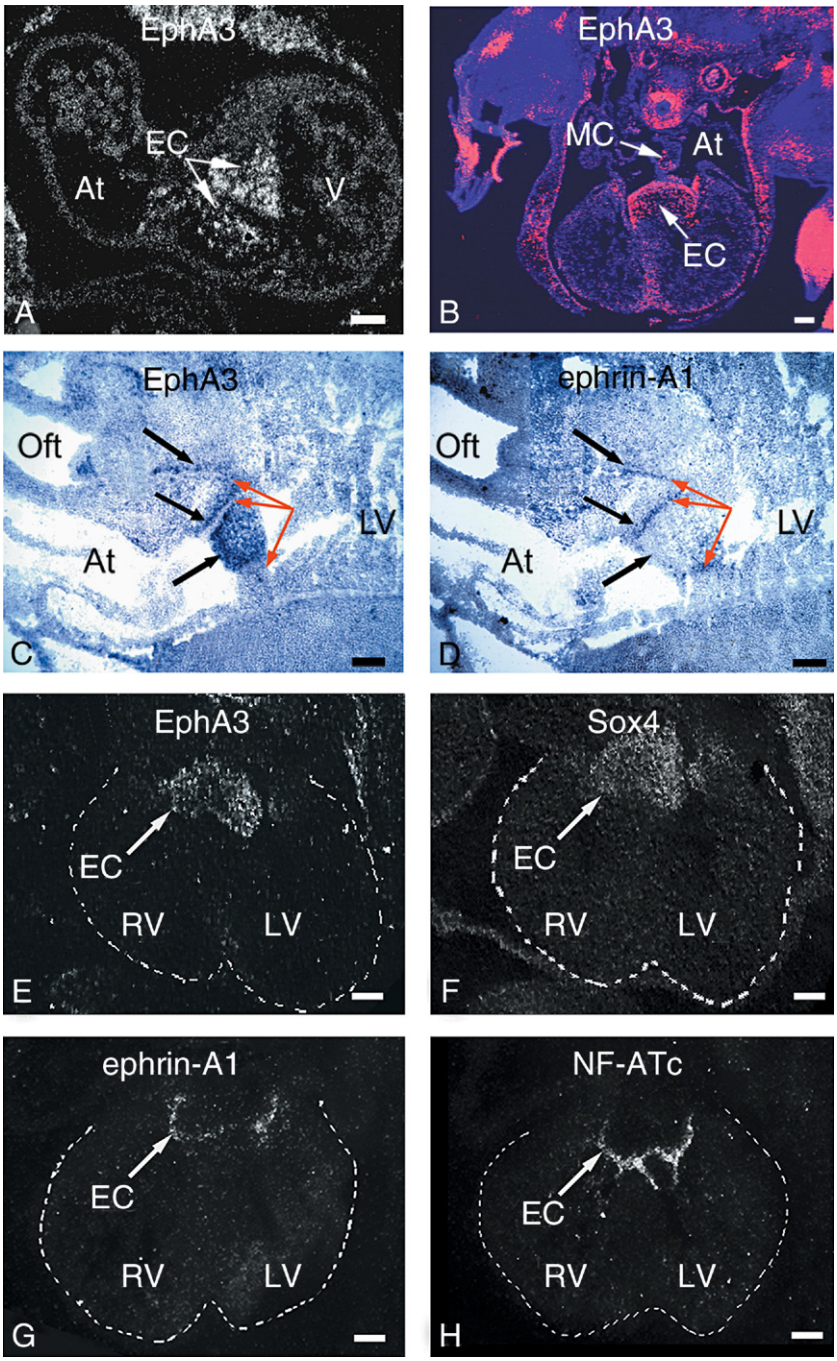

Fig. 3. RNA *in situ* hybridization demonstrates that *EphA3* and *ephrin-A1* are expressed in the developing endocardial cushion tissue. (A) Darkfield micrograph of an E10.5 sagittal section through the heart, after hybridization with an anti-*EphA3* riboprobe. Strong expression is visible in the endocardial cushions of the developing atrioventricular canal. (B) This section, through an E12.5 embryo, is counterstained with DAPI and the silver grains viewed under darkfield illumination with a red filter so that the tissue appears blue while the silver grains, indicating *EphA3* expression, appear red. This RNA *in situ* hybridization demonstrates that *EphA3* is highly expressed in the developing endocardial cushion (EC), and in the mesenchymal cap (MC) on the growing septum primum. (C, D) Serial sagittal sections showing the outflow tract of an E12.5 mouse heart hybridized with anti-sense *EphA3* and *ephrin-A1* digoxigenin-labeled riboprobes. Note that the *ephrin-A1*-expressing cells in panel D (indicated by the red arrows) are directly adjacent to the *EphA3*-expressing cells in panel C (indicated by the black arrows). (E–H) Darkfield illumination of serial cross sections that were hybridized with *EphA3* (E), *Sox4* (F), *ephrin-A1* (G) and *NF-ATc* (H) demonstrate that while *ephrin-A1* is expressed in the *NF-ATc*-positive endothelial lining of the endocardial cushions, *EphA3* is expressed in the adjacent *Sox4*-positive mesenchymal cells. At, atria; EC, endocardial cushion tissue; MC, mesenchymal cap of the growing atrial septum primum; Oft, outflow tract; RV, right ventricle: LV, left ventricle; V, ventricle. Scale bar 0.1 mm.

the ventricular volumes in the same E12.5 *EphA3*$^{-/-}$ and wildtype embryos (Figs.4C, F, I). This analysis demonstrated that there was no significant difference in ventricular volumes between *EphA3*$^{-/-}$ and wildtype hearts.

Delayed fusion of EphA3$^{-/-}$ *endocardial cushions*

In the atrioventricular canal region, both an inferior (dorsal) endocardial cushion and a superior (ventral) endocardial

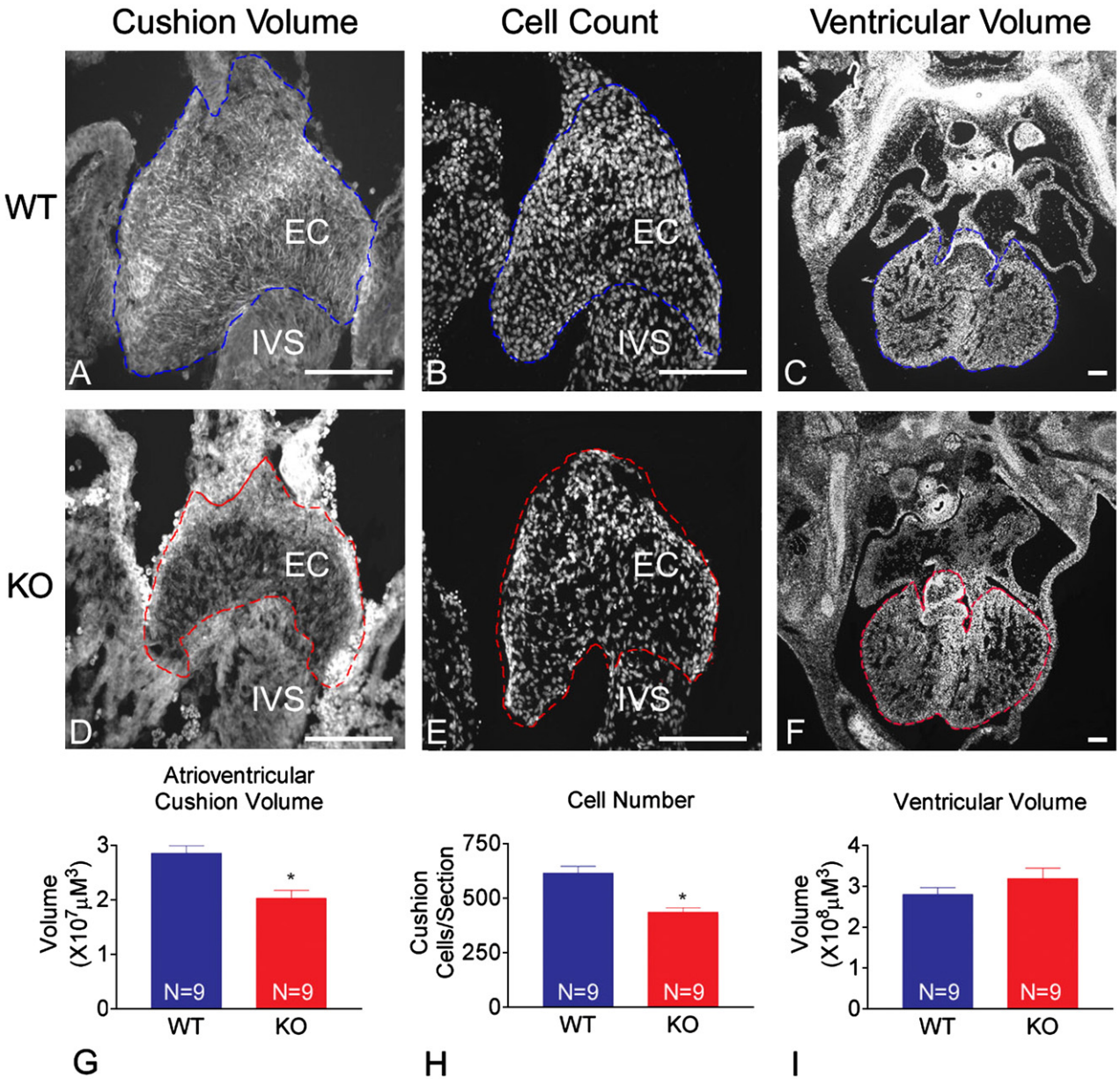

Fig. 4. *EphA3*$^{-/-}$ atrioventricular endocardial cushions are hypoplastic. Histological sections through the entire atrioventricular endocardial cushions of E12.5 wildtype (N=9) and *EphA3*$^{-/-}$ (N=9) embryos were stained with phalloidin–rhodamine to delineate the extent of the cushions in each section (dashed outlines in A, B, D, E) and with DAPI, to delineate cell nuclei. (A, D, G) The average volume of *EphA3*$^{-/-}$ atrioventricular endocardial cushions is 28.8% smaller than wildtype. (B, E, H) Sections from the middle 25% of the endocardial cushions were counterstained with DAPI (after the phalloidin–rhodamine staining) and endocardial cushion cell nuclei counted. The average number of cells per section through the middle of *EphA3*$^{-/-}$ atrioventricular endocardial cushions is 29% lower than wildtype. (C, F, I) The ventricular area (outlined with a dashed line) in each phalloidin–rhodamine-stained section was also measured using Image Pro Plus software and the average ventricular volume of wildtype and *EphA3*$^{-/-}$ hearts calculated. There is no significant difference in ventricular volumes between wildtype and *EphA3*$^{-/-}$ hearts. EC, endocardial cushion tissue; WT, wildtype; KO, *EphA3* knockout; IVS, interventricular septum. Scale bar 0.1 mm.

cushion are formed (van den Hoff et al., 2001). Subsequent growth and fusion of the two cushions produce a central mesenchymal mass by E11.5 in the mouse, which is further remodeled to form the mature mitral and tricuspid valves and atrioventricular septum. Since *EphA3*$^{-/-}$ atrioventricular endocardial cushions are hypoplastic, less tissue is available to span the atrioventricular canal than in wildtype hearts. Thus we predicted that atrioventricular endocardial cushion fusion would be delayed in *EphA3*$^{-/-}$ hearts. On examination, 75% (9/12) of *EphA3*$^{-/-}$ E11.5 atrioventricular endocardial cushions were not yet fused whereas all (14/14) wildtype atrioventricular endocardial cushions were fused by this time (Figs. 5A, B).

EMT and migration in EphA3$^{-/-}$ *endocardial cushions*

Within the atrioventricular canal a subpopulation of endothelial cells undergo an EMT to form the endocardial cushion. During the EMT these cells undergo morphological changes as they lose cell–cell adhesions, extend filopodia and migrate into the extracellular matrix separating the endothelium

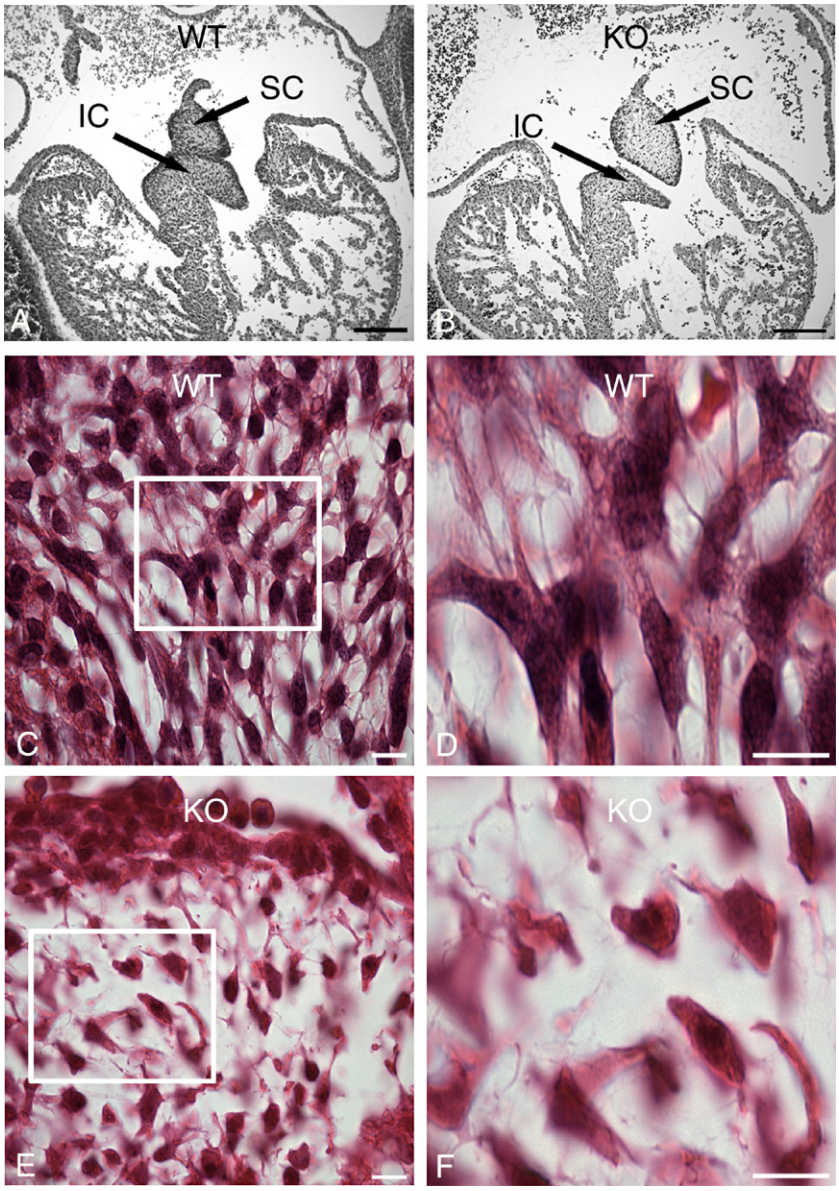

Fig. 5. Atrioventricular endocardial cushion fusion and cellular morphology is abnormal in *EphA3*$^{-/-}$ embryos. (A, B) Hematoxylin and eosin-stained E11.5 wildtype and *EphA3*$^{-/-}$ cross sections demonstrate that there is a delay in atrioventricular endocardial cushion fusion in approximately 75% (9/12) *EphA3*$^{-/-}$ embryos. (C–F) Hematoxylin and eosin-stained E12.5 wildtype and *EphA3*$^{-/-}$ endocardial cushion cells. The areas magnified in panels D and F correspond to the boxed areas in panels C and E, respectively. Note that the wildtype endocardial cushion cells have a flattened morphology with many cellular protrusions and extensions that appear to connect neighboring cells ($N=18$). On the other hand, in 14 of the 18 *EphA3*$^{-/-}$ embryos examined the endocardial cushion cells, appeared rounded-up and to have few cellular extensions. IC, inferior endocardial cushion tissue; SC, superior endocardial cushion tissue; WT, wildtype; KO, *EphA3* knockout. Scale bar in panels A and B, 0.1 mm. Scale bar in panels C–F, 0.01 mm.

and myocardium. (Markwald et al., 1979a). High power histological examination of wildtype atrioventricular endocardial cushions demonstrated flattened cells with multiple processes that were aligned in the same direction and extended to neighboring cells (Figs. 5C, D). *EphA3*$^{-/-}$ atrioventricular endocardial cushion cells, on the other hand, appeared rounded-up with few or no processes (Figs. 5E, F). This abnormal cellular morphology was seen in 78% (14/18) of the E12.5 *EphA3*$^{-/-}$ embryos examined. To further characterize the lack of cellular processes and alignment in *EphA3*$^{-/-}$ endocardial cushion cells we used phalloidin staining of wildtype and *EphA3*$^{-/-}$ sections to visualize filamentous actin (F-actin) (Zhao and Rivkees, 2004). Endocardial cushion cells from E12.5 wildtype embryos exhibited long, well-defined actin stress fibers that aligned with each other in a radial orientation (at approximately right angles to the endocardial cushion surface), whereas endocardial cells from the E12.5 *EphA3*$^{-/-}$ embryos that demonstrated the rounded-up morphology either had fewer stress fibers (weaker phalloidin staining) or stress fibers that were shorter than wildtype and not aligned between cells (Fig. 6).

We used an *ex vivo* explant assay to compare the ability of wildtype and *EphA3*$^{-/-}$ endocardial cushion explants to generate

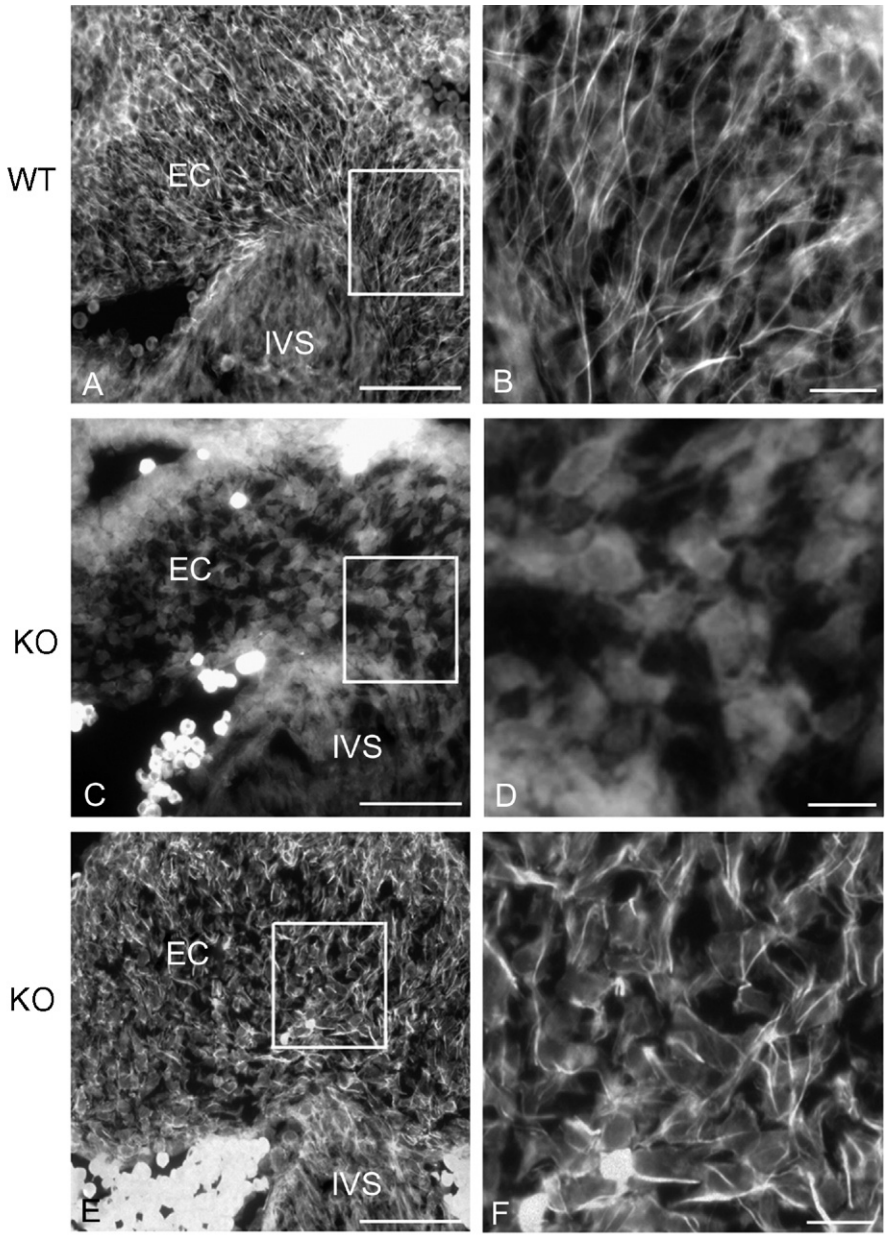

Fig. 6. Stress fibers in *EphA3*$^{-/-}$ endocardial cushion cells are reduced in size and disorganized. Sections of E12.5 wildtype (N=18) and *EphA3*$^{-/-}$ (N=18) hearts were stained with a phalloidin–rhodamine conjugate to reveal the pattern of F-actin in the endocardial cushion cells. (A, B) Stress fibers in wildtype atrioventricular endocardial cushion cells are long, appear almost continuous between cells and to be arranged in a roughly parallel alignment at right angles to the surface of the endocardial cushion. (C, D) In the majority of *EphA3*$^{-/-}$ endocardial cushions stress fibers as evidenced by phalloidin staining could not be demonstrated. (E, F) In the minority of cases in which phalloidin staining revealed stress fibers in *EphA3*$^{-/-}$ endocardial cushion cells the fibers were short and appeared to be oriented randomly relative to the surface of the endocardial cushion and to other endocardial cushion cells. The areas magnified in panels B, D and E correspond to the boxed areas in panels A, C and E respectively. EC, endocardial cushion tissue; IVS, interventricular septum; WT, wildtype; KO, *EphA3* knockout. Scale bar in panels A and C, 0.5 mm. Scale in bar in panels B and D, 0.01 mm.

migrating mesenchymal cells (Bernanke and Markwald, 1979). This assay has been a key tool in the study of EMT in the endocardial cushion (Nakajima et al., 2000). We performed microdissections of E10.5 wildtype (N=16) and *EphA3*$^{-/-}$ (N=12) hearts and separately explanted their ventricles, whole atrioventricular canals and outflow tracts with attached overlying myocardium onto collagen gels. In atrioventricular canal explants, by 48 h a subset of endothelial cells transform into spindle-shaped mesenchymal cells that migrate laterally and invade the collagen gel. Approximately 17± 0.6 and 24±1 wildtype mesenchymal cells migrated into the gel after 48 and 72 h, respectively (Figs. 7A–C). In the *EphA3*$^{-/-}$ atrioventricular canal explants, the number of mesenchymal cells that invaded the collagen gel was significantly reduced (approximately 9±0.5 and 16±0.6 mesenchymal cells were scored after 48 and 72 h, respectively). There was no difference in the number of cells migrating into the collagen gel in wildtype and *EphA3*$^{-/-}$ outflow tract explants and no cells were observed to migrate into the

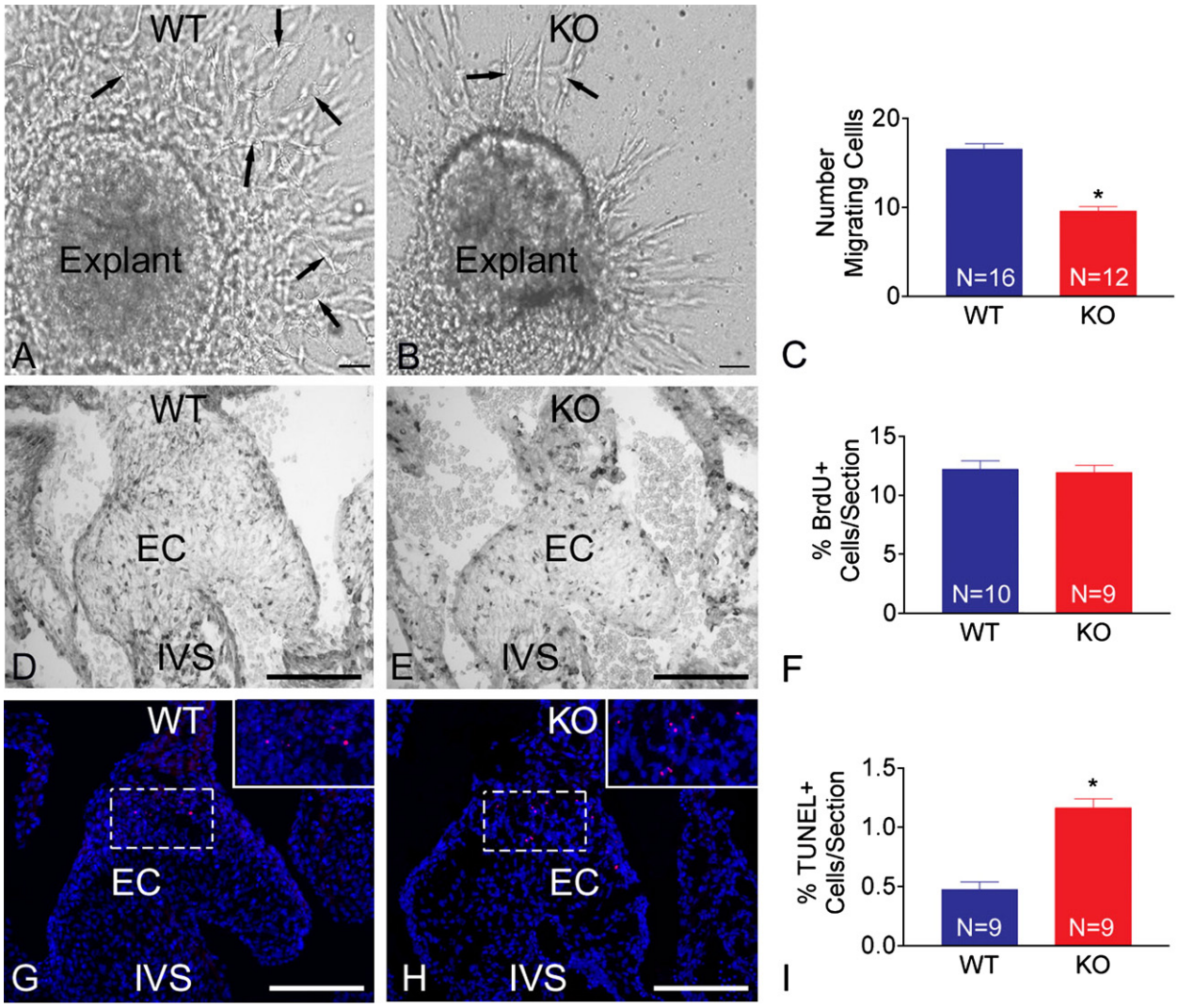

Fig. 7. EMT is reduced in *EphA3*$^{-/-}$ endocardial cushion cells. (A, B, C) Endocardial cushion explants from E10.5 (A) wildtype ($N=16$) and (B) KO ($N=12$) embryos were seeded onto type I collagen gels and the number of cells migrating into the collagen gel scored. The migrating cells were beneath the surface of the gel and had a typical spin-shaped appearance (arrows). There are significantly fewer migrating cells scored in *EphA3*$^{-/-}$ endocardial cushion explants (Student's *t*-test, $P<0.05$). (D, E, F) Proliferating cells were identified in sections of wildtype ($N=10$) and *EphA3*$^{-/-}$ ($N=9$) atrioventricular endocardial cushions by BrdU incorporation. Cells in the S-phase of mitosis were identified by anti-BrdU immunohistochemistry using a DAB reaction. There is no significant difference in the number of BrdU-labeled endocardial cushion cells between wildtype and *EphA3*$^{-/-}$ embryos. (G, H, I) Cells undergoing apoptosis were identified in sections of wildtype ($N=9$) and *EphA3*$^{-/-}$ ($N=9$) atrioventricular endocardial cushions by TUNEL staining. The sections were counterstained with DAPI to facilitate scoring of apoptotic nuclei. Insets in panels G and H are approximately 2-fold magnifications of the boxed regions in these panels. Almost all apoptotic nuclei were confined to the medial region of the endocardial cushion where the atrial septum fuses with the central mesenchymal mass. The percentage of apoptotic nuclei though low was greater in this region in *EphA3*$^{-/-}$ endocardial cushions compared to wildtype (Student's *t*-test, $P<0.05$). EC, endocardial cushion tissue; IVS, interventricular septum; WT, wildtype; KO, *EphA3* knockout. Scale bar 0.1 mm.

collagen gel in negative control wildtype and *EphA3*$^{-/-}$ ventricular explants (data not shown).

Proliferation and apoptosis in EphA3$^{-/-}$ *atrioventricular endocardial cushions*

We have shown that the E12.5 atrioventricular endocardial cushions and the structures they give rise to, the atrioventricular valves and septa, are underdeveloped in *EphA3*$^{-/-}$ embryos and neonates. While their reduction in size might be attributed wholly to EMT and migration abnormalities in the developing atrioventricular endocardial cushions, decreased proliferation and/or increased apoptosis in *EphA3*$^{-/-}$ endocardial cushion cells could also be contributing factors. To investigate these possibilities we compared the levels of BrdU incorporation and the number of TUNEL-positive cells, in wildtype and *EphA3*$^{-/-}$ endocardial cushions at E11.5 and E12.5, respectively. *In vivo* BrdU labeling did not reveal any significant difference in cell proliferation between *EphA3*$^{-/-}$ ($N=9$) and wildtype ($N=10$) E12.5 atrioventricular endocardial cushions (Figs. 7D, E, F). The average percentage of TUNEL-positive cell per section through the middle 25% of *EphA3*$^{-/-}$ atrioventricular endocardial cushions was significantly greater than wildtype ($1.2\pm 0.08\%$ versus $0.49\pm 0.07\%$ TUNEL-positive cells per section,

$N=9$ for each genotype). In keeping with previous descriptions of apoptosis in atrioventricular endocardial cushions (Abdelwahid et al., 2002), the TUNEL-positive cells were almost exclusively confined to the medial portion of the endocardial cushion where the atrial septum attaches to the central mesenchymal mass (Figs. 7G, H).

Discussion

Cause of death in EphA3$^{-/-}$ mice

The histopathology we describe indicates that *EphA3*$^{-/-}$ mice die of pulmonary edema due to elevated cardiac filling pressures. These elevated filling pressures are evidenced by the blood congestion in *EphA3*$^{-/-}$ atria, lungs, and livers. Ventricular failure is an unlikely explanation for the high cardiac filling pressures and atrial dilatation, since the *EphA3*$^{-/-}$ animals are normally formed at birth and mouse mutants with ventricular failure typically die at midgestation due to forward failure (Srivastava and Olson, 1996). Furthermore, while *EphA3*$^{-/-}$ ventricles are histologically indistinguishable from those of wildtype animals, *EphA3*$^{-/-}$ atrioventricular valves and septal structures are obviously abnormal compared to wildtype. These structures are derived from the *EphA3*-expressing endocardial cushions.

The *EphA3*$^{-/-}$ atrioventricular valves have dilated annuli and their valve leaflets give the appearance of being inadequate to close off the atrioventricular canals. The atrioventricular cushion-derived septum bridges the interatrial and interventricular septa through fusion (Harvey, 2002). In the *EphA3*$^{-/-}$ mutant hearts this septal area is hypoplastic which may account for the annular dilatation of their atrioventricular canals. Annular dilatation is itself a well-known cause of valvular dysfunction (Gillinov and Cosgrove, 2002). Incompetent atrioventricular valves in *EphA3*$^{-/-}$ mice would account for their atrial enlargement and increased cardiac filling pressure. Pulmonary congestion in *EphA3*$^{-/-}$ embryos might be kept low because embryonic lungs are collapsed and their vascular resistance is correspondingly high. However at birth, as the lungs begin to inflate, pulmonary vascular resistance rapidly falls. This falling resistance along with elevated cardiac filling pressure would rapidly lead to pulmonary edema, due in part to the unprepared nature of neonatal lung vasculature. Similar complications have been noted in newborn humans with incompetent mitral valves (Grifka and Vincent, 1998).

EphA3$^{-/-}$ mice were found to have significant bradycardia (HR = 297 ± 17.9 bpm versus 396 ± 16.3 bpm in wildtype) and a first degree AV block, as evidenced by the prolonged PR interval (0.06 ± 0.006 s compared to 0.04 ± 0.005 s in wildtype mice). The wildtype heart rate and PR interval values are comparable to reported standards (Chaves et al., 2003; McGuire and Alexander, 1993). The first degree heart block could reflect AV node dysfunction secondary to abnormal endocardial cushion development (Smits et al., 2005) or alternatively these conduction defects could simply be a feature of the terminally failing heart. Importantly, electrocardiograph analyses did not reveal evidence of arrhythmia or of second- or third-degree AV conduction block. Thus, it is unlikely that perinatal death in *EphA3*$^{-/-}$ mice is attributable to conduction defects.

EphA3 signaling in development of the atrial septum

The atrial septum develops as an outgrowth from the roof of the primitive atrium. This outgrowth, the septum primum, grows toward the atrioventricular endocardial cushion starting at E9 in the mouse (Harvey, 2002; Webb et al., 1998). The leading edge of the septum primum is composed of a thickened mesenchymal cap. The expression of *EphA3* in the mesenchymal cap of the growing septum primum, and the dysgenesis of the septum primum, together suggest that *EphA3* signaling is required for the directed growth and development of this structure. The large atrial septal defects seen in *EphA3*$^{-/-}$ mice probably contribute to their cyanosis but are almost certainly not as central to their perinatal death as are their incompetent atrioventricular valves and the resulting pulmonary edema.

EphA3 signaling in endocardial cushion development

The primitive heart tube consists of an inner layer of endocardial cells and an outer layer of myocardial cells, separated by a layer of extracellular matrix material referred to as cardiac jelly (Eisenberg and Makrwald, 1995; Icardo and Manasek, 1992). Endocardial cushions begin as bulges of cardiac jelly, and arise within two regions in the primitive heart tube: the atrioventricular canal and the ventricular outflow tract. Thereafter, the endothelial cells lining the cushions undergo EMT and migrate into the cardiac jelly swellings. This ordered morphogenesis separates the common atrioventricular canal into left and right atrioventricular canals, and gives rise to the atrioventricular valves, the atrioventricular and membranous interventricular septa, and contributes (along with neural crest cells) to the semilunar valves of the outflow tracts (Icardo and Manasek, 1992; Markwald et al., 1979a, 1977; Olson and Srivastava, 1996).

Our observation that *EphA3*$^{-/-}$ mice have developmental defects in their atrioventricular valves and atrial septum, is consistent with the early expression of *EphA3* in the atrioventricular endocardial cushion tissue and the mesenchymal cap of the septum primum. While *EphA3* is also expressed in the outflow tract cushion tissue, examination of *EphA3*$^{-/-}$ mutant outflow tracts did not reveal any abnormalities (data not shown). The greater pathology in the atrioventricular valves is presumably due to the fact that the semilunar valves are derived from both endocardial cushions and from neural crest cells whereas the atrioventricular valves are derived from their endocardial cushions alone (Kisanuki et al., 2001; Nishibatake et al., 1987).

Our analyses clearly show that the abnormalities in *EphA3*$^{-/-}$ valves and septa can be traced back to defective development of the atrioventricular endocardial cushions. We have shown that there are reduced numbers of mesenchymal cells in *EphA3*$^{-/-}$ atrioventricular endocardial cushions and that these cushions are underdeveloped. We suggest that the reduced size of the

atrioventricular endocardial cushion without a proportional reduction in the overall size of the heart (the wildtype and *EphA3*$^{-/-}$ ventricular volumes were not significantly different from one another) renders the mesenchymal mass in the center of the heart insufficient to form competent valves and septa. This would explain the delayed fusion of the inferior and superior atrioventricular endocardial cushions in *EphA3*$^{-/-}$ embryos and the apparent annular dilatation in P0 *EphA3*$^{-/-}$ mice.

Cellular mechanisms of EphA3 action in endocardial cushion development

Our demonstration that *EphA3*$^{-/-}$ endocardial cushion explants have a significant reduction in the number of cells that migrate into the collagen gel suggests that the reduced number of mesenchymal cells in *EphA3*$^{-/-}$ endocardial cushions is due to reduced capacity of these cells to delaminate from the endothelial lining and migrate into the cardiac jelly. Since increased apoptosis or decreased proliferation could also contribute to the reduced number of cells in *EphA3*$^{-/-}$ endocardial cushions, we analyzed apoptosis and proliferation in wildtype and *EphA3*$^{-/-}$ atrioventricular endocardial cushions. These analyses revealed a slight increase in the percentage of endocardial cushion cells undergoing apoptosis in *EphA3*$^{-/-}$ endocardial cushions. However, given the overall very low number of endocardial cushion cells undergoing apoptosis in *EphA3*$^{-/-}$ endocardial cushions we feel it unlikely that apoptosis accounts for the *EphA3*$^{-/-}$ phenotype. The more dramatic reduction in cell migration demonstrated in the *EphA3*$^{-/-}$ endocardial cushion explants provides a much more plausible explanation for the *EphA3*$^{-/-}$ defects.

Molecular mechanisms of EphA3$^{-/-}$ *action in endocardial cushion development*

We have shown that *EphA3* and its ligand, *ephrin-A1*, are expressed in groups of cells in close proximity to each other in the developing endocardial cushions and that there are histological and functional defects in the atrioventricular septal structures that they form. We suggest that as endothelial cells undergo the transition to a mesenchymal phenotype they lose their *ephrin-A1* expression and begin to express *EphA3*. The loss of ephrin expression may decrease cell adhesiveness (as ephrin-A5 activation has been shown to increase cell adhesiveness (Davy and Robbins, 2000; Huai and Drescher, 2001)) and allow these cells to detach from the endothelial layer. This process might be aided by the concomitant expression of EphA3 in these cells, which would further decrease integrin-mediated cell attachments (as has been shown for EphA2 activation (Miao et al., 2000)). Furthermore, since in most cases, EphA–ephrin-A interactions mediate repulsive signals (Flanagan and Vanderhaeghen, 1998; Holder and Klein, 1999; Noren and Pasquale, 2004; Wilkinson, 2000), the EphA3-expressing endocardial cushion cells undergoing EMT may be repelled by the ephrin-A1-expressing endothelial cushion cells and migrate into the cardiac jelly. If an endothelial cell undergoing EMT were to experience a repulsive signal from the cells that surround it in the plane of the endothelial lining, then the net repulsive force would be directed at right angels to the endothelial lining. Thus the EphA3–ephrin-A1 interaction may explain the roughly parallel alignment of the long axes of the mesenchymal cells in the cardiac jelly at right angels to the endothelial lining of the endocardial cushion. The lack of EphA3 signaling in the *EphA3*$^{-/-}$ atrioventricular endocardial cushions may therefore explain the decreased number of endocardial cushion cells undergoing EMT and the abnormal alignment of the mesenchymal cells that do migrate into the cardiac jelly.

The Rho family of small GTPases are among the best documented downstream targets of EphA receptor signaling (Kullander and Klein, 2002; Murai and Pasquale, 2003; Noren and Pasquale, 2004). Rho family GTPases, typified by Rho, Rac and cdc42, have been shown to be key regulatory proteins of cell morphology and migration promoting the formation of stress fibers (Rho), lamellipodia (Rac) and filopodia (cdc42) (Nobes and Hall, 1995). Attempts to demonstrate Rho activation in endocardial cushion cells were unsuccessful due to the poor protein yields from such small structures however we suggest that the disorganization and near-absence of stress fibers in the majority of *EphA3*$^{-/-}$ endocardial cushion cells may be due to decreased Rho activity.

It is interesting to consider why perinatal mortality is only partially penetrant in *EphA3*$^{-/-}$ pups. TGFβ, which has long been known to stimulate endocardial cushion EMT (Camenisch et al., 2002; Nakajima et al., 2000), has been shown to signal through Rho to effect EMT in a variety of cell types (Bhowmick et al., 2001; Kaartinen et al., 2002; Masszi et al., 2003). Thus we suggest that a critical threshold of Rho activation is necessary for endocardial cushion cells to undergo EMT and that both TGFβ and EphA3 signaling contribute to Rho activation. We hypothesize that in the absence of EphA3, Rho activation reaches this critical threshold in fewer endocardial cushion cells and therefore fewer cells undergo EMT. The incomplete penetrance of mortality in the *EphA3*$^{-/-}$ mice may therefore be explained by stochastic variation in the number of endocardial cushion cells reaching the required level of Rho activation necessary for EMT in different *EphA3*$^{-/-}$ embryos.

In summary, the critical role of EphA3 in cardiac development is confirmed by the severe cardiac malformations observed in the *EphA3* knockouts. The morphogenetic events in endocardial cushion development depend on sustained signals that induce cell migration and differentiation (Eisenberg and Makrwald, 1995). Though contact guidance and chemotaxis have been implicated in the control of cushion cell migration (Markwald et al., 1979a, 1979b), no candidate molecules controlling this directed cell movement have been put forward nor have genes essential to the development of the atrial septum yet been identified. We have shown that *EphA3* and *ephrin-A1* are expressed in complementary patterns in the endocardial cushions and atrial septa and that *EphA3* null mutants have abnormalities in the development of these structures. Our results therefore demonstrate that EphA3 signaling is a critical

mediator of the morphogenetic signals that control endocardial cushion and atrial septa development.

Acknowledgments

This work was supported by grants from The Heart and Stroke Foundation of Canada (A.B.) and from the NIH of the United States (G.L.). Amy Fawkes was supported by an OGSST (Ontario Graduate Scholarship Science Technology) award. Dr. A. Brown is supported by a New Investigator Award from the Heart and Stroke Foundation of Canada. We would like to thank Dr. G. Pickering, Dr. H. Rosenberg for their helpful discussions concerning the *EphA3*$^{-/-}$ cardiac phenotype. We would also like to thank Denis Gris and Kelly Galloway-Kay for the technical assistance.

References

Abdelwahid, E., Pelliniemi, L.J., Jokinen, E., 2002. Cell death and differentiation in the development of the endocardial cushion of the embryonic heart. Microsc. Res. Tech. 58, 395–403.

Abercrombie, M., 1946. Estimation of nuclear population from microtome sections. Anat. Rec. 94, 239–247.

Adams, R., Wilkinson, G., Weiss, C., Diella, F., Gale, N., Deutsch, U., Risau, W., Klein, R., 1999. Roles of ephrinB ligands and ephB receptors in cardiovascular development: demarcation of arterial/venous domains vascular morphogenesis, and sprouting angiogenesis. Genes Dev. 13, 295–306.

Bernanke, D.H., Markwald, R.R., 1979. Effects of hyaluronic acid on cardiac cushion tissue cells in collagen matrix cultures. Tex. Rep. Biol. Med. 39, 271–285.

Bernanke, D.H., Markwald, R.R., 1982. Migratory behavior of cardiac cushion tissue cells in a collagen-lattice culture system. Dev. Biol. 91, 235–245.

Bhowmick, N.A., Ghiassi, M., Bakin, A., Aakre, M., Lundquist, C.A., Engel, M.E., Arteaga, C.L., Moses, H.L., 2001. Transforming growth factor-beta1 mediates epithelial to mesenchymal transdifferentiation through a RhoA-dependent mechanism. Mol. Biol. Cell 12, 27–36.

Boyd, A.W., Lackmann, M., 2001. Signals from Eph and ephrin proteins: a developmental tool kit. Sci STKE RE20.

Brown, A., Yates, P.A., Burrola, P., Ortuno, D., Vaidya, A., Jessell, T.M., Pfaff, S.L., O'Leary, D.D., Lemke, G., 2000. Topographic mapping from the retina to the midbrain is controlled by relative but not absolute levels of EphA receptor signaling. Cell 102, 77–88.

Camenisch, T.D., Molin, D.G., Person, A., Runyan, R.B., Gittenberger-de Groot, A.C., McDonald, J.A., Klewer, S.E., 2002. Temporal and distinct TGFbeta ligand requirements during mouse and avian endocardial cushion morphogenesis. Dev. Biol. 248, 170–181.

Chaves, A.A., Dech, S.J., Nakayama, T., Hamlin, R.L., Bauer, J.A., Carnes, C.A., 2003. Age and anesthetic effects on murine electrocardiography. Life Sci. 72, 2401–2412.

Cooke, J.E., Moens, C.B., 2002. Boundary formation in the hindbrain: Eph only it were simple. Trends Neurosci. 25, 260–267.

Cregan, S.P., MacLaurin, J.G., Craig, C.G., Robertson, G.S., Nicholson, D.W., Park, D.S., Slack, R.S., 1999. Bax-dependent caspase-3 activation is a key determinant in p53-induced apoptosis in neurons. J. Neurosci. 19, 7860–7869.

Davis, S., Gale, N.W., Aldrich, T.H., Maisonpierre, P.C., Lhotak, V., Pawson, T., Goldfarb, M., Yancopoulos, G.D., 1994. Ligands for EPH-related receptor tyrosine kinases that require membrane attachment or clustering for activity. Science 266, 816–819.

Davy, A., Robbins, S.M., 2000. Ephrin-A5 modulates cell adhesion and morphology in an integrin-dependent manner. EMBO J. 19, 5396–5405.

Drescher, U., Kremoser, C., Handwerker, C., Loschinger, J., Noda, M., Bonhoeffer, F., 1995. In vitro guidance of retinal ganglion cell axons by RAGS, a 25 kDa tectal protein related to ligands for Eph receptor tyrosine kinases. Cell 82, 359–370.

Eisenberg, L., Makrwald, R., 1995. Molecular regulation of atrioventricular vavuloseptal morphogenesis. Circ. Res. 77, 1–6.

Flanagan, J.G., Vanderhaeghen, P., 1998. The ephrins and Eph receptors in neural development. Annu. Rev. Neurosci. 21, 309–345.

Gale, N., Yancopoulos, G., 1997. Ephrins and their receptors: a repulsive topic. Cell Tissue Res. 290, 227–241.

Gale, N., Valenzuela, D., Flenniken, A., Pan, L., Ryan, T., Henkemeyer, M., Strebhardt, K., Hirai, H., Wilkinson, D., Pawson, T., Yancopoulos, G., 1996. Eph receptors and ligands comprise two major specificity subclasses and are reciprocally compartmentalized during embryogenesis. Neuron 17, 9–19.

Gilardi-Hebenstreit, P., Nieto, M., Frain, M., Mattei, M., Chestier, A., Wilkinson, D., Charnay, P., 1992. An Eph-related receptor protein tyrosine kinase gene segmentally expressed in the developing mouse hindbrain. Oncogene 7, 2499–2506.

Gillinov, A.M., Cosgrove, D.M., 2002. Mitral valve repair for degenerative disease. J. Heart Valve Dis. 11 (Suppl. 1), S15–S20.

Grifka, R.G., Vincent, J.A., 1998. Abnormalities of the left atrium and mitral valve, including mitral valve prolapse. In: Garson, A., Bricker, J.T., Fisher, D.J., Neish, S.R. (Eds.), The Science and Practise of Pediatric Cardiology. Williams and Wilkins, Baltimore, pp. 1277–1302.

Harvey, R.P., 2002. Organogenesis: patterning the vertebrate heart. Nat. Rev., Genet. 3, 544–556.

Holder, N., Klein, R., 1999. Eph receptors and ephrins: effectors of morphogenesis. Development 126, 2033–2044.

Holmberg, J., Clarke, D.L., Frisen, J., 2000. Regulation of repulsion versus adhesion by different splice forms of an Eph receptor. Nature 408, 203–206.

Huai, J., Drescher, U., 2001. An ephrin-A-dependent signaling pathway controls integrin function and is linked to the tyrosine phosphorylation of a 120-kDa protein. J. Biol. Chem. 276, 6689–6694.

Icardo, J., Manasek, F., 1992. Cardiogenesis: development mechanisms and embryology. In: Fozzard, H. (Ed.), The Heart and Cardiovascular System Second Edition. Raven Press, New York, pp. 1563–1586.

Kaartinen, V., Haataja, L., Nagy, A., Heisterkamp, N., Groffen, J., 2002. TGFbeta3-induced activation of RhoA/Rho-kinase pathway is necessary but not sufficient for epithelio-mesenchymal transdifferentiation: implications for palatogenesis. Int. J. Mol. Med. 9, 563–570.

Kilpatrick, T.J., Brown, A., Lai, C., Gassmann, M., Goulding, M., Lemke, G., 1996. Expression of the Tyro4/Mek4/Cek4 gene specifically marks a subset of embryonic motor neurons and their muscle targets. Mol. Cell. Neurosci. 7, 62–74.

Kisanuki, Y.Y., Hammer, R.E., Miyazaki, J., Williams, S.C., Richardson, J.A., Yanagisawa, M., 2001. Tie2-Cre transgenic mice: a new model for endothelial cell-lineage analysis in vivo. Dev. Biol. 230, 230–242.

Klein, R., 2001. Excitatory Eph receptors and adhesive ephrin ligands. Curr. Opin. Cell Biol. 13, 196–203.

Knoll, B., Drescher, U., 2002. Ephrin-As as receptors in topographic projections. Trends Neurosci. 25, 145–149.

Knoll, B., Zarbalis, K., Wurst, W., Drescher, U., 2001. A role for the EphA family in the topographic targeting of vomeronasal axons. Development 128, 895–906.

Krull, C.E., 1998. Inhibitory interactions in the patterning of trunk neural crest migration. Ann. N. Y. Acad. Sci. 857, 13–22.

Krull, C., Lansford, R., Gale, N., Collazo, A., Marcelle, C., Yancoupolus, G., Fraser, S., Bronner-Fraser, M., 1997. Interactions of Eph-related receptors and ligands confer rostrocaudal pattern to trunk neural crest migration. Curr. Biol. 7, 571–580.

Kullander, K., Klein, R., 2002. Mechanisms and functions of Eph and ephrin signalling. Nat. Rev., Mol. Cell Biol. 3, 475–486.

Lawrenson, I.D., Wimmer-Kleikamp, S.H., Lock, P., Schoenwaelder, S.M., Down, M., Boyd, A.W., Alewood, P.F., Lackmann, M., 2002. Ephrin-A5 induces rounding, blebbing and de-adhesion of EphA3-expressing 293T and melanoma cells by CrkII and Rho-mediated signalling. J. Cell Sci. 115, 1059–1072.

Marco, J.Y., Schilham, M.W., de Boer, P.A.J., Moorman, A.F.M., Clevers, H., Lamers, W.H., 1998. Sox4-deficiency syndrome in mice is an animal model for common trunk. Circ. Res. 83, 986–994.

Markwald, R., Fitzharris, T., Manasek, F., 1977. Structure and development of endocardial cushions. Am. J. Anat. 148, 85–120.

Markwald, R., Fitzharris, T., Bolender, D., Bernanke, D., 1979a. Structural analysis of cell:matrix interaction during morphogenesis of atrioventricular cushion tissue. Dev. Biol. 69, 634–654.

Markwald, R., Funderberg, F., Bernanke, D., 1979b. Glycosaminoglycans: potential determinates in cardiac morphogenesis. Tex. Rep. Biol. Med. 39, 253–270.

Masszi, A., Di Ciano, C., Sirokmany, G., Arthur, W.T., Rotstein, O.D., Wang, J., McCulloch, C.A., Rosivall, L., Mucsi, I., Kapus, A., 2003. Central role for Rho in TGF-beta1-induced alpha-smooth muscle actin expression during epithelial–mesenchymal transition. Am. J. Physiol.: Renal. Physiol. 284, F911–F924.

McGuire, P.G., Alexander, S.M., 1993. Inhibition of urokinase synthesis and cell surface binding alters the motile behavior of embryonic endocardial-derived mesenchymal cells in vitro. Development 118, 931–939.

Mellitzer, G., Xu, Q., Wilkinson, D., 1999. Eph receptors and ephrins restrict cell intermingling and communication. Nature 400, 77–81.

Miao, H., Burnett, E., Kinch, M., Simon, E., Wang, B., 2000. Activation of EphA2 kinase suppresses integrin function and causes focal-adhesion-kinase dephosphorylation. Nat. Cell Biol. 2, 62–69.

Murai, K.K., Pasquale, E.B., 2003. 'Eph'ective signaling: forward, reverse and crosstalk. J. Cell Sci. 116, 2823–2832.

Nakajima, Y., Yamagishi, T., Hokari, S., Nakamura, H., 2000. Mechanisms involved in valvuloseptal endocardial cushion formation in early cardiogenesis: roles of transforming growth factor (TGF)-beta and bone morphogenetic protein (BMP). Anat. Rec. 258, 119–127.

Naruse-Nakajima, C., Asano, M., Iwakura, Y., 2001. Involvement of EphA2 in the formation of the tail notochord via interaction with ephrinA1. Mech. Dev. 102, 95–105.

Nishibatake, M., Kirby, M.L., Van Mierop, L.H., 1987. Pathogenesis of persistent truncus arteriosus and dextroposed aorta in the chick embryo after neural crest ablation. Circulation 75, 255–264.

Nobes, C.D., Hall, A., 1995. Rho, rac and cdc42 GTPases: regulators of actin structures, cell adhesion and motility. Biochem. Soc. Trans. 23, 456–459.

Noren, N.K., Pasquale, E.B., 2004. Eph receptor-ephrin bidirectional signals that target Ras and Rho proteins. Cell. Signal. 16, 655–666.

Olson, E., Srivastava, D., 1996. Molecular pathways controlling heart development. Science 272, 671–676.

Pompa, J.d.l., Timmerman, L., Takimoto, H., Yoshida, H., Elia, A., Samper, E., Potter, J., Wakeham, A., Marengere, L., Langille, B., Crabtree, G., Mak, T., 1998. Role of the NF-ATc transcription factor in morphogenesis of cardiac valves and septum. Nature 392, 182–185.

Ranger, A., Brusby, M., Hodge, M., Bravallese, E., Brousse, F.d.l., Hoey, T., Mickanin, C., Baldwin, H., Glimcher, L., 1998. The transcription factor NF-ATc is essential for cardiac valve formation. Nature 392, 186–190.

Runyan, R.B., Markwald, R.R., 1983. Invasion of mesenchyme into three-dimensional collagen gels: a regional and temporal analysis of interaction in embryonic heart tissue. Dev. Biol. 95, 108–114.

Schaeren-Wiemers, N., Gerfin-Moser, A., 1993. A single protocol to detect transcripts of various types and expression levels in neural tissue and cultured cells: in situ hybridization using digoxigenin-labeled cRNA probes. Histochemistry 100, 431–440.

Smith, A., Robinson, V., Patel, K., Wilkinson, D., 1997. The EphA4 and EphB1 receptor tyrosine kinases and ephrin-B2 ligand regulate targeted migration of branchial neural crest cells. Curr. Biol. 7, 561–570.

Smits, J.P., Veldkamp, M.W., Wilde, A.A., 2005. Mechanisms of inherited cardiac conduction disease. Europace 7, 122–137.

Srivastava, D., Olson, E., 1996. Neurotrophin-3 knocks heart off Trk. Nat. Med. 2, 1069–1071.

Vaidya, A., Pniak, A., Lemke, G., Brown, A., 2003. EphA3 null mutants do not demonstrate motor axon guidance defects. Mol. Cell. Biol. 23, 8092–8098.

van den Hoff, M.J., Kruithof, B.P., Moorman, A.F., Markwald, R.R., Wessels, A., 2001. Formation of myocardium after the initial development of the linear heart tube. Dev. Biol. 240, 61–76.

Webb, S., Brown, N., Anderson, R., 1998. Formation of the atrioventricular septal structures in the normal mouse. Circ. Res. 82, 645–656.

Wilkinson, D.G., 2000. Eph receptors and ephrins: regulators of guidance and assembly. Int. Rev. Cytol. 196, 177–244.

Winslow, J., Moran, P., Valverde, J., Shih, A., Yuan, J., Wong, S., Tsai, S., Goddard, A., Henzel, W., Hefti, F., Beck, K., Caras, I., 1995. Cloning of AL-1, a ligand for an Eph-related tyrosine kinase receptor involved in axon bundle formation. Neuron 14, 973–981.

Xu, Q., Mellitzer, G., Robinson, V., Wilkinson, D., 1999. In vivo cell sorting in complementary segmental domains mediated by Eph receptors and ephrins. Nature 399, 267–271.

Zhao, Z., Rivkees, S.A., 2004. Rho-associated kinases play a role in endocardial cell differentiation and migration. Dev. Biol. 275, 183–191.